

## Nonthermal Melting of a Charge Density Wave in $\text{TiSe}_2$

E. Möhr-Vorobeva,<sup>1</sup> S. L. Johnson,<sup>1</sup> P. Beaud,<sup>1</sup> U. Staub,<sup>1</sup> R. De Souza,<sup>1</sup> C. Milne,<sup>1,2</sup> G. Ingold,<sup>1</sup> J. Demsar,<sup>3</sup>  
H. Schaefer,<sup>3</sup> and A. Titov<sup>4</sup>

<sup>1</sup>*Swiss Light Source, Paul Scherrer Institut, CH-5232 Villigen, Switzerland*

<sup>2</sup>*Laboratoire de Spectroscopie Ultrarapide, EPFL, 1015 Lausanne, Switzerland*

<sup>3</sup>*Physics Department and Center of Applied Photonics, University of Konstanz, Germany*

<sup>4</sup>*Institute of Metal Physics and Institute of Metallurgy UrDRAS, Ekaterinburg, Russia*

(Received 22 February 2011; published 14 July 2011)

We use time-resolved optical reflectivity and x-ray diffraction with femtosecond resolution to study the dynamics of the structural order parameter of the charge density wave phase in  $\text{TiSe}_2$ . We find that the energy density required to melt the charge density wave nonthermally is substantially lower than that required for thermal suppression and is comparable to the charge density wave condensation energy. This observation, together with the fact that the structural dynamics take place on an extremely fast time scale, supports the exciton condensation mechanism for the charge density wave in  $\text{TiSe}_2$ .

DOI: 10.1103/PhysRevLett.107.036403

PACS numbers: 71.45.Lr, 61.05.C-, 78.47.J-

Recent developments in time-resolved techniques such as angle-resolved photoemission spectroscopy and x-ray diffraction have opened new opportunities to probe directly the dynamics of electronic [1] and structural [2] order on femtosecond time scales. Charge density waves (CDWs) [3] comprise a class of collective phenomena arising from a correlation between the electron density and the underlying lattice.  $1T\text{-TiSe}_2$  is a controversial example of a CDW material. It has a quasi-two-dimensional crystal structure where Ti atoms are sandwiched between two layers of Se atoms [see Fig. 1(b)]. Below  $T_c \approx 200$  K, it undergoes a second-order structural phase transition into a commensurate CDW with a  $(2a \times 2a \times 2c)$  superlattice (SL).  $\text{TiSe}_2$  can be intercalated with transition metal ions which reside between the layers. The recent discovery of superconductivity in  $\text{Cu}_x\text{TiSe}_2$  below 2.3 K [4] has intensified interest in the host compound.

The origin of the CDW phase transition in  $\text{TiSe}_2$ , although extensively studied both experimentally and theoretically, is not yet unambiguously determined. Lack of parallel areas in the Fermi surface at  $2k_F$  eliminates Fermi surface nesting as a possible scenario for the CDW formation [5,6]. There exist several competing hypotheses for the mechanism driving the CDW formation in  $1T\text{-TiSe}_2$ . One of the most promising is the condensation of excitons [7], which becomes possible due to a low free carrier density and a consequently poorly screened Coulomb interaction. An alternative is the band Jahn-Teller effect: a lowering of the average energy of the valence and conduction bands in the vicinity of the Fermi surface as a result of lattice distortion [8,9]. A variety of experiments, including measurements of the electronic band structure via angle-resolved photoemission, have been interpreted in different ways to support both models [6,10]. For a qualitative description of the angle-resolved photoemission data

[10], hybrid exciton-phonon modes driving the transition were proposed [11].

One possible way to distinguish between these mechanisms is to study the dynamics of the CDW phase in response to the strong, sudden electronic excitation resulting from the absorption of a femtosecond laser pulse. Although all models for the CDW mechanism predict a collapse of the SL, differences in the expected threshold energy and recovery dynamics provide a way to discriminate between them. In this Letter, we discuss the laser-induced structural dynamics studied with transient x-ray diffraction and optical reflectivity. With x-ray diffraction we access directly the atomic rearrangement in the material after the perturbation of electrons with a femtosecond laser pulse and investigate the fluence dependence of the structural order in  $\text{TiSe}_2$ . In addition, high time resolution and precision available from transient optical reflectivity measurements provide detailed information on temperature and fluence dependence of the phonon mode associated with the CDW phase.

For the transient optical reflectivity measurements, the output of a commercial Ti:sapphire laser (800 nm, 290 kHz, 40–100 fs) was used to produce both pump and probe pulse trains. The induced transient reflectivity signal was collected by using a fast-scan technique [12]. The probe beam was polarized along the crystal  $\mathbf{a}$  axis, and the polarization of the pump was set to  $45^\circ$  with respect to the probe, both incident nearly normal to the (001) sample surface. The pump beam was focused to a  $100 \mu\text{m}$  spot, and the probe was a factor of 2 smaller in diameter to ensure homogeneous excitation of the probe region.

Figure 1(a) shows the temperature dependence of the transient optical reflectivity signal at a pump fluence of  $3 \mu\text{J}/\text{cm}^2$ . At low temperatures the data reveal the presence of oscillations with a frequency of approximately

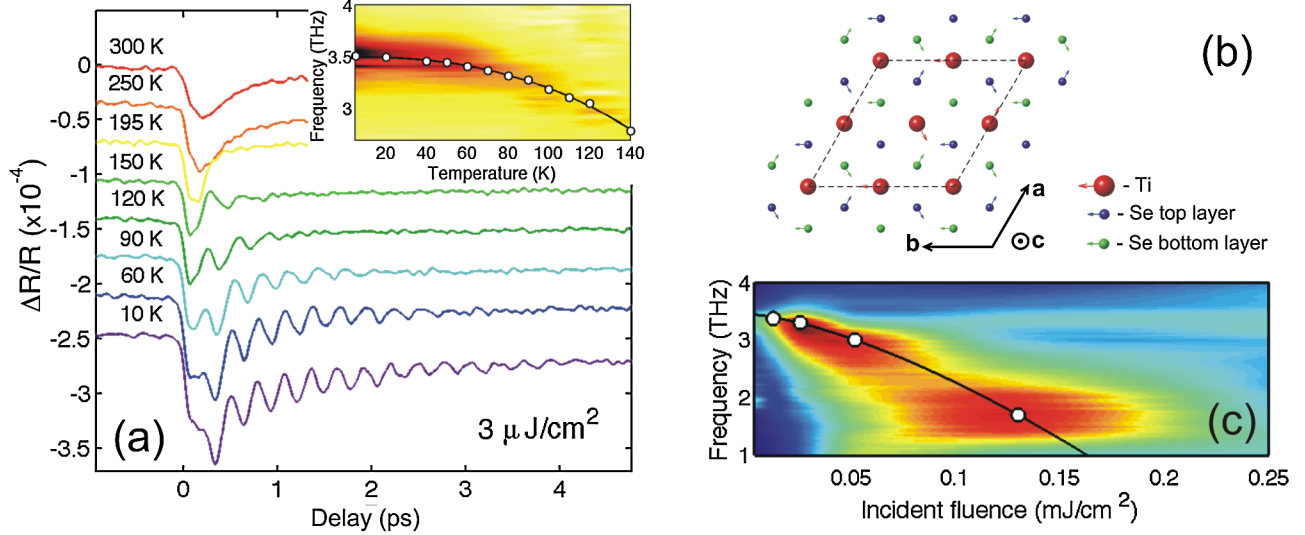


FIG. 1 (color online). (a) Temperature dependence of the transient reflectivity signal of  $\text{TiSe}_2$  measured at a laser fluence of  $3 \mu\text{J}/\text{cm}^2$ . The inset shows the power spectrum of the oscillatory component of the data and the peak positions as extracted from a fit to a damped oscillator model. (b)  $\text{TiSe}_2$  unit cell at  $T < T_c$ . Arrows indicate the atomic displacements associated with the  $A_{1g}$  amplitude mode of the CDW phase [22]. (c) Power spectrum of the oscillatory part of the reflectivity measured at  $T = 80 \text{ K}$  for different excitation fluences. Open circles indicate peak positions of the  $A_{1g}$  mode of the CDW.

3.4 THz. As the temperature increases, the frequency decreases [inset in Fig. 1(a)] and the damping increases. There is no evidence of oscillations at temperatures above 170 K. Based on Raman spectroscopic data [13,14], we assign these oscillations to the  $A_{1g}$  amplitude mode of the CDW. The atomic displacements associated with this mode are shown with arrows in Fig. 1(b). The frequency of the  $A_{1g}$  mode depends strongly on laser fluence. Figure 1(c) shows the Fourier transform of the oscillatory part of the fluence dependence data taken at 80 K. At an incident pump fluence of  $0.21 \text{ mJ}/\text{cm}^2$  the  $A_{1g}$  mode is completely suppressed, suggesting the collapse of the CDW phase. This corresponds to an absorbed energy of 16.5 meV per temperature (RT) unit cell, as calculated with a penetration depth of 18 nm and a reflectivity of 65% [15].

To extract more quantitative information on the structural dynamics, we performed transient x-ray diffraction measurements, using the intensity of the  $(\frac{1}{2} \frac{1}{2} \frac{1}{2})$  SL peak as a measure of structural order in the CDW phase. The measurements were done in a grazing incidence geometry [16] with 140 fs FWHM x-ray pulses generated by the laser-electron beam slicing technique [17]. The x-ray beam was focused to  $\approx 6 \mu\text{m}$  vertically and  $250 \mu\text{m}$  horizontally. To reduce the fluorescence background, the x-ray energy was set below the Ti  $K$ -edge absorption to 4.9 keV, by using a multilayer mirror with a 1.3% bandwidth acceptance. At a grazing angle of  $(0.67 \pm 0.02)^\circ$ , the attenuation length of the 4.9 keV x rays is  $(58 \pm 5) \text{ nm}$ . Approximately 150 fs FWHM laser pulses with  $\lambda = 1580 \text{ nm}$  excited the sample at normal incidence. The estimated laser penetration depth at 1580 nm is 35 nm [15]. This is significantly larger than for 800 nm light and matches better with the probe depth of the x rays.

To maintain the time resolution of the experiment to within 250 fs, we tilted the pulse front of the pump laser by  $45^\circ$  by imaging the first-order reflection of a 600 lines/mm grating onto the sample [18,19]. The laser spot size was  $(810 \times 840) \mu\text{m}^2$  FWHM.

Figure 2 shows the time evolution of the diffraction signal following photoexcitation at 90 and 140 K. Laser-induced perturbation of the electronic order in  $\text{TiSe}_2$  in the CDW phase results in atomic rearrangement and hence in a change in the SL diffraction peak intensity. At low pump fluences the diffraction signal drops rapidly and recovers on a picosecond time scale, whereas at high fluences the

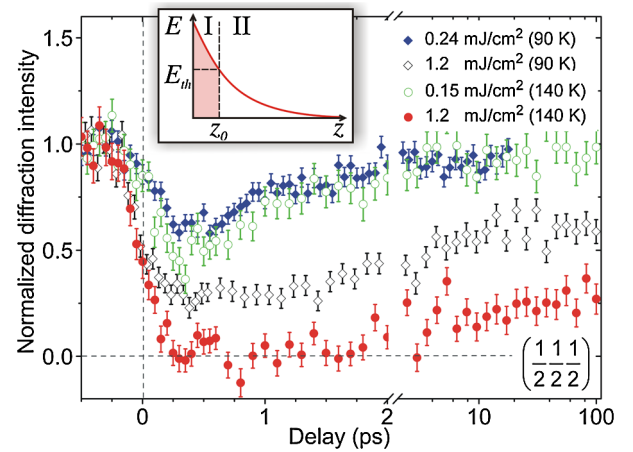


FIG. 2 (color online). Time evolution of the  $(\frac{1}{2} \frac{1}{2} \frac{1}{2})$  diffraction peak after laser excitation at 90 and 140 K. The inset shows laser excitation energy per u.c. in the sample vs distance from the sample surface. Regions I and II correspond to melted and perturbed CDW phases, respectively.

recovery time increases dramatically. At 140 K with an incident excitation density of  $1.2 \text{ mJ/cm}^2$ , the SL order vanishes completely within our experimental time resolution of 250 fs, indicating a phase transition to the normal state over the entire probed volume. The signal recovers partially on a time scale of about 10 ps. A complete recovery of the initial state occurs approximately 100 ns later. In order to qualitatively describe the fluence-dependent data, we suggest the following picture (see the inset in Fig. 2). Assuming linear absorption, the laser excitation density decays exponentially with the distance  $z$  from the surface. Provided that the excitation is sufficiently strong, there will exist a depth  $z_0$  at which the laser energy absorbed within a u.c. volume is just enough to suppress the SL order:  $E(z_0) = E_{\text{th}}$ . For  $z < z_0$  (region I), the CDW order is completely suppressed, and the material undergoes a phase transition to a high symmetry state. For  $z > z_0$  (region II), the CDW is only perturbed from its initial state at  $T_0$ , but the SL order still persists with a reduced amplitude. The recovery of the SL order in these two regions of the sample are determined by distinct physical processes. In region II, the initial recovery is governed by the time required for the electronic subsystem to transfer energy to the lattice. For region I, where the CDW order was completely suppressed, a significant amount of additional time is required for CDW domain regrowth, since it involves the establishment of long-range structural correlations. At low laser fluences, the excitation level is insufficient to melt the CDW. As the fluence increases over a certain threshold, the melted region I appears, growing with increasing fluence. At the highest excitation fluence of  $1.2 \text{ mJ/cm}^2$  at  $T_0 = 140 \text{ K}$ , the CDW order is suppressed over the entire probe volume. The observed recovery dynamics at high laser fluence is then dominated by the much slower CDW domain regrowth. This picture is supported by the shape of the rocking curves measured at a 100 ps delay for different excitation levels. At a laser fluence of  $0.2 \text{ mJ/cm}^2$ , for an initial temperature of 90 K the data show no angular broadening of the diffraction peak, indicating that the correlation length is unchanged [20]. At an excitation level of  $1.2 \text{ mJ/cm}^2$ , the diffraction peak becomes 2.2 times broader with respect to the unpumped signal at both 90 and 140 K, indicating a reduced correlation length in the probe volume.

To determine the energy required to melt the CDW phase, we measured the fluence dependence of the SL diffraction peak intensity at a 100 ps delay. For these measurements we used 70 ps FWHM x-ray pulses as a probe. The energy was set to 4.9 keV by using a Si(111) monochromator with 0.015% bandwidth.

Figure 3 shows the normalized  $(\frac{1}{2} \frac{1}{2} \frac{1}{2})$  diffraction peak intensity vs incident laser fluence at 90 and 140 K. The drop in SL peak intensity shows a clear threshold, which indicates the onset of the CDW melting and depends on the initial temperature of the sample. On a 100 ps time scale, the electronic and lattice subsystems are expected to be in

quasiequilibrium at a somewhat elevated temperature. Therefore, some portion of the fluence-dependent drop in the SL diffraction peak intensity can be attributed to the laser-induced heating of the sample. This thermal effect can be estimated by using the temperature-dependent specific heat [21], the laser reflectivity of 60%, and the laser penetration depth of 35 nm at 1580 nm [15]. We estimate that a temperature increase in the probe volume at the highest incident fluence of  $1.2 \text{ mJ/cm}^2$  is 46 and 56 K for initial temperatures of 140 and 90 K, respectively. These are the upper limits for the estimates of the thermal effect, as we do not take into account heat diffusion from the probe volume. To estimate the corresponding change in structure factor of the  $(\frac{1}{2} \frac{1}{2} \frac{1}{2})$  SL diffraction peak, we use the atomic displacements associated with the SL [Fig. 1(b)], which we calculate from the temperature dependence of the  $(\frac{3}{2} \frac{1}{2} \frac{1}{2})$  neutron diffraction peak intensity [22]. This, in turn, allows us to estimate the change of the  $(\frac{1}{2} \frac{1}{2} \frac{1}{2})$  x-ray diffraction peak intensity as a function of temperature. The maximum thermal contributions as a function of incident laser fluence at 140 and 90 K are shown in Fig. 3 with gray lines. At a maximum pump fluence of  $1.2 \text{ mJ/cm}^2$ , the thermally induced reduction of the SL diffraction intensity (in the absence of diffusion) is  $\approx 50\%$  for 140 K and  $\approx 30\%$  for 90 K. A complete suppression of the CDW phase due to laser-induced heating would require an energy of  $E_{\text{th}}^T(T_0) = \int_{T_0}^{T_c} C_p(T) dT$ , where  $C_p$  is the specific heat [21]. Thus, calculated thermal threshold energies for one RT unit cell are  $E_{\text{th}}^T(140 \text{ K}) = 36.7 \text{ meV}$  and  $E_{\text{th}}^T(90 \text{ K}) = 60.0 \text{ meV}$ . This, together with the observation of a threshold behavior, rules out the thermal origin of the CDW suppression. We argue that the threshold is a result of melting of the CDW in region I. As suggested by the time dependence of the diffraction

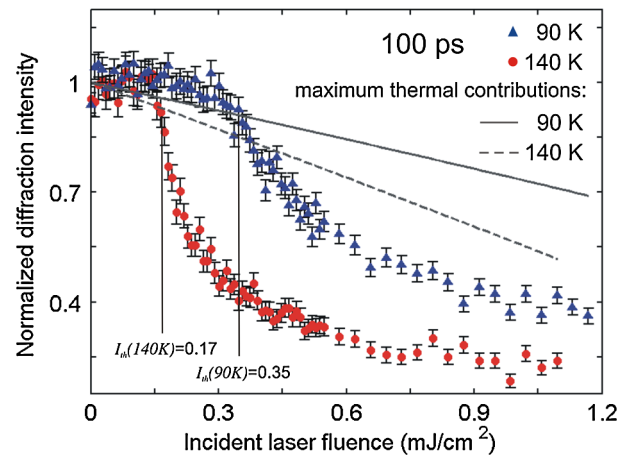


FIG. 3 (color online). Normalized intensity of the  $(\frac{1}{2} \frac{1}{2} \frac{1}{2})$  SL peak at 100 ps after excitation vs incident laser fluence at 140 K (●) and 90 K (▲). The threshold fluences ( $I_{\text{th}}$ ) are determined from the extrema of the numerical derivatives of the curves. Gray lines correspond to the calculated maximum thermal contribution to the drop in the diffraction intensity.



TABLE I. Comparison of the electron condensation energy  $E_{\text{con}}$ , the threshold energy required to suppress the superlattice  $E_{\text{th}}^S$ , and the threshold energy for thermal melting of the CDW phase  $E_{\text{th}}^T$ . All the values are calculated for one RT unit cell.

	$E_{\text{con}}$ (meV)	$E_{\text{th}}^S$ (meV)	$E_{\text{th}}^T$ (meV)
140 K	5.7	7.9	36.7
90 K	9.0	15.8	60.0

intensity (Fig. 2), on a 100 ps time scale the long-range structural correlation in the portion of the crystal initially driven through the phase transition (region I) has not yet been fully reestablished. This causes an additional drop of the SL peak intensity due to the reduced correlation length. The experimentally observed threshold fluences (Fig. 3) are 0.17 mJ/cm<sup>2</sup> at 140 K and 0.35 mJ/cm<sup>2</sup> at 90 K, corresponding to threshold energy densities of  $E_{\text{th}}(140 \text{ K}) = 7.9 \text{ meV}$  and  $E_{\text{th}}(90 \text{ K}) = 15.8 \text{ meV}$ , respectively. These are much lower than the energy densities required to heat up the sample to  $T_c$  (Table I) and consistent with the value of 16.5 meV determined from the optical reflectivity data at 80 K.

It is instructive to compare the energy density required to suppress the SL to the total condensation energy of the CDW phase,  $E_{\text{con}}$ . As there is no easy way to estimate  $E_{\text{con}}$  for either excitonic insulator or band Jahn-Teller-type ground states, we make a crude comparison to a 1D-Peierls system, where the condensation energy is given by  $E_{\text{con}} = n(\epsilon_F) \cdot \Delta^2/2$  [Eq. (3.45) in Ref. [3]]. In this expression,  $n(\epsilon_F)$  is the normal state density of states and  $\Delta$  is the size of a single particle gap. If the lattice modulation in the CDW phase is driven directly by the electronic subsystem, as in the case of the excitonic insulator model, the amount of energy of  $E_{\text{con}}$  absorbed selectively by the electronic subsystem should be sufficient to drive the material to the normal state. At low temperatures ( $T \lesssim 10 \text{ K}$ ), an estimate for the size of the gap size is  $\Delta_0 \approx 150 \text{ meV}$  [23]. If the gap follows the mean-field curve  $\Delta(T) = \Delta_0 \sqrt{1 - (T/T_c)^2}$ , then  $\Delta(90 \text{ K}) = 134 \text{ meV}$  and  $\Delta(140 \text{ K}) = 107 \text{ meV}$ . The density of states per unit cell at the Fermi level in the normal phase is  $n(\epsilon_F) = 1 \text{ eV}^{-1}$  [24]. The condensation energies thus obtained are  $E_{\text{con}}(90 \text{ K}) = 9.0 \text{ meV}$  and  $E_{\text{con}}(140 \text{ K}) = 5.7 \text{ meV}$ . Although slightly lower than the measured thresholds for laser-induced CDW melting, they are quite similar (see Table I). This observation is at odds with recent results on a standard Peierls quasi-1D CDW  $\text{K}_{0.3}\text{MoO}_3$  [12]. In this system, the energy required for the laser-induced suppression of the zone-folded modes is an order of magnitude higher than the electronic part of the total condensation energy, which is larger than  $E_{\text{con}}$  by the increased amount of the elastic energy of the lattice.

By combining time-resolved optical reflectivity and x-ray diffraction, we have shown that the laser-induced melting of the CDW phase occurs on a time scale faster than 250 fs and requires 4 times less energy than expected

for suppression by only heat deposition of the pump laser. This stands in contrast to previous studies of the laser-induced superlattice suppression in 1D CDW  $\text{K}_{0.3}\text{MoO}_3$  [12] and 2D CDW  $\text{TaS}_2$  [25] systems, where the thermal and laser-driven thresholds are similar. This, coupled with the similarity of the experimentally determined threshold for SL suppression and the CDW condensation energy, gives experimental evidence for an electronic origin of the CDW formation in  $\text{TiSe}_2$ , as hypothesized by the exciton condensate scenario.

The transient x-ray diffraction measurements were performed on the X05LA beam line at the Swiss Light Source, Paul Scherrer Institut, Villigen, Switzerland. Optical experiments were done at the University of Konstanz, Germany. We thank C. Monney for helpful discussion and acknowledge financial support from the Swiss National Foundation through the NCCR MUST, MaNEP, and from the Alexander von Humboldt foundation.

- 
- [1] F. Schmitt *et al.*, *Science* **321**, 1649 (2008).
  - [2] P. Beaud *et al.*, *Phys. Rev. Lett.* **103**, 155702 (2009).
  - [3] G. Grüner, in *Density Waves in Solids*, edited by D. Pines (Addison-Wesley, Reading, MA, 1994).
  - [4] E. Morosan *et al.*, *Nature Phys.* **2**, 544 (2006).
  - [5] A. Zunger and A.J. Freeman, *Phys. Rev. B* **17**, 1839 (1978).
  - [6] K. Rossmagel, L. Kipp, and M. Skibowski, *Phys. Rev. B* **65**, 235101 (2002).
  - [7] J.A. Wilson, *Solid State Commun.* **22**, 551 (1977); C. Monney *et al.*, *Phys. Rev. B* **79**, 045116 (2009); *Phys. Rev. Lett.* **106**, 106404 (2011).
  - [8] H.P. Hughes, *J. Phys. C* **10**, L319 (1977).
  - [9] M.H. Whangbo and E. Canadell, *J. Am. Chem. Soc.* **114**, 9587 (1992).
  - [10] H. Cercellier *et al.*, *Phys. Rev. Lett.* **99**, 146403 (2007).
  - [11] J. vanWezel, P. Nahai-Williamson, and S.S. Saxena, *Phys. Rev. B* **81**, 165109 (2010).
  - [12] A. Tomeljak *et al.*, *Phys. Rev. Lett.* **102**, 066404 (2009).
  - [13] C.S. Snow *et al.*, *Phys. Rev. Lett.* **91**, 136402 (2003).
  - [14] J.A. Holy, K.C. Woo, M.V. Klein, and F.C. Brown, *Phys. Rev. B* **16**, 3628 (1977).
  - [15] S.C. Bayliss and W.Y. Liang, *J. Phys. C* **18**, 3327 (1985).
  - [16] S.L. Johnson *et al.*, *Phys. Rev. Lett.* **100**, 155501 (2008).
  - [17] P. Beaud *et al.*, *Phys. Rev. Lett.* **99**, 174801 (2007).
  - [18] J. Hebling, *Opt. Quantum Electron.* **28**, 1759 (1996).
  - [19] P. Baum and A.H. Zewail, *Proc. Natl. Acad. Sci. U.S.A.* **103**, 16 105 (2006).
  - [20] The rocking curve at low excitation fluence at 140 K was not measured.
  - [21] R. Craven, F. DiSalvo, and F. Hsu, *Solid State Commun.* **25**, 39 (1978).
  - [22] F.J. DiSalvo, D.E. Moncton, and J.V. Waszczak, *Phys. Rev. B* **14**, 4321 (1976).
  - [23] G. Li *et al.*, *Phys. Rev. Lett.* **99**, 027404 (2007).
  - [24] Y. Yoshida and K. Motizuki, *J. Phys. Soc. Jpn.* **49**, 898 (1980).
  - [25] M. Eichberger *et al.*, *Nature (London)* **468**, 799 (2010).